



AMERICAN METEOROLOGICAL SOCIETY

Weather and Forecasting

EARLY ONLINE RELEASE

This is a preliminary PDF of the author-produced manuscript that has been peer-reviewed and accepted for publication. Since it is being posted so soon after acceptance, it has not yet been copyedited, formatted, or processed by AMS Publications. This preliminary version of the manuscript may be downloaded, distributed, and cited, but please be aware that there will be visual differences and possibly some content differences between this version and the final published version.

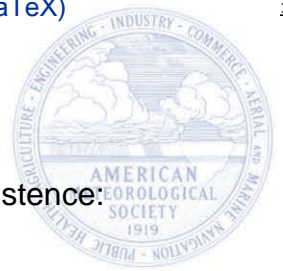
The DOI for this manuscript is doi: 10.1175/WAF-D-18-0027.1

The final published version of this manuscript will replace the preliminary version at the above DOI once it is available.

If you would like to cite this EOR in a separate work, please use the following full citation:

Knaff, J., C. Sampson, and K. Musgrave, 2018: Statistical tropical cyclone wind radii prediction using climatology and persistence: Updates for the western North Pacific. *Wea. Forecasting*. doi:10.1175/WAF-D-18-0027.1, in press.

© 2018 American Meteorological Society



1 Statistical tropical cyclone wind radii prediction using climatology and persistence:
2 Updates for the western North Pacific

3
4 John A. Knaff*

5 *NOAA Center for Satellite Applications and Research*
6 *Fort Collins, Colorado*

7
8 Charles R. Sampson

9 *Naval Research Laboratory*
10 *Monterey, California*

11
12 and

13
14 Kate D. Musgrave

15 *The Cooperative Institute for Research in the Atmosphere*
16 *Fort Collins, Colorado*

17
18
19
20 Prepared for *Weather and Forecasting*
21

22
23
24
25
26
27
28
29 *Corresponding Author: John Knaff, NOAA/NESDIS/RAMMB, Colorado State University,

30 Campus Delivery 1375, Fort Collins, CO 80523-1375, John.Knaff@noaa.gov

31

Abstract

32 This note describes an updated tropical cyclone vortex climatology for the western
33 North Pacific version of the operational wind radii climatology and persistence (i.e.,
34 CLIPER) model. The update addresses known shortcomings of the existing formulation,
35 namely that the wind radii used to develop the original model were too small and
36 symmetric. The underlying formulation of the CLIPER model has not changed, but the
37 larger and more realistic vortex climatology produces improved forecast biases. Other
38 applications that make use of the vortex climatology and CLIPER model forecasts
39 should also benefit from the bias improvements.

40

41 1. Introduction

42 The U.S. tropical cyclone (TC) warning centers provide information about TC surface
43 wind structure – analyzed and forecasted in terms of wind radii. The collective term
44 wind radii refers to the maximum radial extent of TC winds exceeding three critical wind
45 speed thresholds in compass quadrants about the storm center: northeast, southeast,
46 southwest and northwest. The critical wind speed thresholds used at the centers are
47 34, 50, and 64 knots [kt; 1 kt = 0.514 ms⁻¹]; referred to in this paper as R34, R50, and
48 R64, respectively. The U.S. TC warning centers also report and forecast their wind radii
49 in units of nautical miles [n mi; 1 n mi = 1.85 km], and so we use the units kt and n mi
50 throughout this work.

51 Prior to 2005, forecast guidance for wind radii was considered to be unskillful and of
52 marginal use in operations (Knaff et al. 2007a). Around that time, a simple statistical
53 wind radii forecast guidance based on CLImatology and PERsistence (CLIPER) was
54 developed (Knaff et al. 2007b; K07 hereafter). The development of this “wind radii
55 CLIPER model” or “DRCL” (the four letter technique name in the Automated Tropical
56 Cyclone Forecast System: Sampson and Schrader 2000) was part of a larger effort to
57 provide probabilistic forecast information for wind speeds associated with TCs in the
58 North Atlantic and North Pacific (DeMaria et al. 2009; DeMaria et al. 2013). At that
59 time, the developers were confident that satellite-based ocean wind vectors influenced
60 wind radii estimation and best tracking, as indicated in the following statement in K07:

61 *“During this period, operational centers used several satellite-derived products (low-*
62 *level atmospheric motion vectors, passive microwave, and scatterometry) in their*
63 *wind radii estimates. We do not consider these data to be as accurate as the data*

64 *influenced by aircraft reconnaissance; nevertheless, we use these wind radii*
65 *datasets and accept their inherent shortcomings.”*

66 While this turned out to be true in the basins where the National Hurricane Center
67 (NHC) and Central Pacific Hurricane Centers (CPHC) were responsible, this was not
68 the case in the western North Pacific. In hindsight, the western North Pacific wind radii
69 in the best tracks¹ were based on very few observations, mostly fortuitous scatterometer
70 winds and surface observations that were available just prior to the forecaster’s real-
71 time estimates. The resulting DRCL model derived for the western North Pacific, which
72 used those real-time estimates, used a climatological vortex that was too small and
73 symmetric. In this note, we describe how three years of objective wind radii best tracks,
74 which closely match subjectively-determined wind radii best tracks described in
75 Sampson et al. (2017), are used to re-derive the DRCL model used in the western North
76 Pacific. The model updates described in this note are now in operations at the Joint
77 Typhoon Warning Center (JTWC) and serve as both guidance and the skill baseline for
78 TC wind radii forecasts in the western North Pacific.

79 This update contains a brief summary of the data and methods used for model re-
80 derivation, noting that the methods have not changed from K07. We then provide
81 coefficients derived for the new version of DRCL, and examine how these differ from the
82 coefficients in the original K07 version. This is followed by a discussion of how the new

¹ Although wind radii dating back to 1996 can be found in the western North Pacific best tracks, they had not been analyzed post-season until just recently and only for the years 2013-2016 (Edward Fukada, Personal communication, 2017).

83 DRCL formulation works, how it differs from the older version of the model, and its
84 potential impact on operations at JTWC.

85 2. Data and model update

86 a. Updated climatology

87 Three years, 2014 to 2016, of objectively estimated wind radii best tracks were used
88 as input data for creating a climatological dataset. The objective wind radii best track
89 procedures and verification versus a subjectively determined best track are discussed in
90 Sampson et al. (2017). The focus of Sampson et al. (2017) was on 34-kt wind radii
91 estimation in operations. These estimates made use of the available wind radii
92 estimates and helped forecasters more efficiently, systematically, and accurately
93 estimate real-time 34-kt wind radii. An equally weighted mean (or consensus) of real-
94 time objectively determined 34-kt wind radii estimates created a t=0 estimate of wind
95 radii. The inputs to the t=0 consensus included wind radii based on routine Dvorak fixes
96 and matching imagery (i.e., Knaff et al. 2016), microwave sounders (i.e., Demuth et al.
97 2006), the NESDIS multi-satellite-platform surface wind analysis-based fix (Knaff et al.
98 2011), and six-hour forecasts of wind radii from the Global Forecast System, the
99 Hurricane Weather Research and Forecasting model, and the Geophysical Fluid
100 Dynamics Laboratory hurricane model. Sampson et al. (2017) created a 2-yr (2014–15)
101 34-kt wind radii objective analysis using this method. These objective estimates were
102 shown to compare favorably to independently-analyzed wind radii estimates contained
103 in the National Hurricane Center’s postseason estimates (i.e., the best tracks) and a
104 specially created subjectively-analyzed best-track dataset for the western North Pacific.

105 In K07 the average west Pacific R34 was 115 n mi, while in Sampson et al. (2017) the
 106 post-season analyzed R34 was 134 n mi.

107 The method used here is the same as in K07 and starts with a generalized version
 108 of the modified Rankine vortex that includes a wavenumber one asymmetry (1). The
 109 wind, V , is a function of radius (r) and azimuth (θ), and x is the shape parameter, a is
 110 the asymmetry, θ_o is the azimuthal orientation, v_m is the maximum wind in the vortex,
 111 and r_m is the radius of maximum wind.

$$\begin{aligned}
 112 \quad V(r, \theta) &= (v_m - a) \left(\frac{r_m}{r} \right)^x + a \cos(\theta - \theta_o) \quad \text{for } r \geq r_m \\
 V(r, \theta) &= (v_m - a) \left(\frac{r}{r_m} \right) + a \cos(\theta - \theta_o) \quad \text{for } r < r_m
 \end{aligned} \tag{1}$$

113 The four free parameters (i.e., x , a , θ_o , and r_m) in (1) are climatological values of
 114 parameters found in the best track (latitude, storm translational speed, and storm
 115 maximum winds) as shown in (2). The climatological values are all denoted with the
 116 subscript “c”, and t_0 - t_2 , a_0 - a_3 , x_0 - x_2 , and m_0 - m_2 are all constants.

$$117 \quad \left. \begin{cases} \theta_{oc} = t_0 + t_1\gamma + t_2c \\ a_c = a_0 + a_1c + a_2c^2 + a_3\gamma \\ x_c = x_0 + x_1v_m + x_2\gamma \\ r_{mc} = m_0 + m_1v_m + m_2\gamma \end{cases} \right\}, \text{ where } \left. \begin{cases} \gamma \equiv \text{Latitude} - 25. \\ c \equiv \text{Storm Speed} \\ v_m \equiv \text{maximum wind} \end{cases} \right\} \tag{2}$$

118 The choice of this functional form approximates known variations in tropical cyclone
 119 structure. Azimuthal orientation of asymmetries can be affected by interaction with the
 120 background environment and here is a function of latitude and translation speed (c).
 121 Asymmetries are prescribed to be a function of translational speed and latitude – the

122 justification of which is discussed in Uhlhorn et al. (2014), and Klotz and Jiang (2016).
123 Tropical cyclone size, which is represented by the shape parameter x , is both a function
124 of intensity (TCs grow larger as they become more intense) and latitude (TCs grow
125 larger as they move poleward; see Knaff et al. 2014, Merrill 1984, and Weatherford and
126 Gray 1988). Finally, r_{mc} in (2) is a function of latitude and intensity, following Knaff et al.
127 (2015) and references therein. Allowing r_{mc} to vary with latitude and intensity provides
128 even more variability in the model. For instance, wind radii can be increased simply by
129 assigning a larger value of r_{mc} . One shortcoming of this added variability is that the r_{mc}
130 values are typically unrealistically large when compared to observed radii of maximum
131 wind.

132 The parametric vortex defined in (1) and (2) has 13 free parameters, and there is no
133 unique set of 13 parameters that would fit a single set of wind radii values in the best
134 track. Instead, the 13 parameters are chosen to minimize the RMS errors of the
135 observed R34, R50 and R64 from a large sample of cases. Because the vortex profile
136 is a nonlinear function of the parameters, there are probably local minima in the RMS
137 error function. It is also likely that some values of the parameters can lead to solutions
138 that are not physically realistic, so penalty terms are employed in the error function to
139 restrict the solutions to physically realistic values. This process is similar to the method
140 of steepest descent first published by Debye (1909). In our algorithm, only one
141 parameter at a time is varied over a range of physically realistic values to avoid the
142 need for a closed form of the gradient of the error function with respect to the thirteen
143 parameters. The details of this methodology follow.

144 Input and output variables in (2) are scaled so that they are of order one. This
145 scaling strategy is the more elegant of the two methods discussed in K07. The scaling
146 factors used were 30 kt, 1, 100 n mi, and 90° for a_c , x_c , r_{mc} , and θ_{oc} , and 165 kt, 50° , and
147 30 kt for v_m , γ , and c , which are based on near maximum values in the best tracks.
148 Because we use this scaling, the search increment for each variable is comparable to
149 the other variables. As previously mentioned, vortex parameters are physically
150 constrained by applying a penalty term to the error function, i.e., the RMS difference
151 between the estimated and observed radii. The penalty term increases the RMSE for
152 these cases by multiplying the amount vortex parameters are out of range by a large
153 coefficient (10^6). The RMSEs with the penalty term act as a loss function, for which we
154 seek a minimum. This method allows the searching algorithm to consider coefficients
155 where vortex parameters are out of range for a few cases, but results in vortex
156 parameters that do not violate physical constraints. For instance, values of $x > 1.0$
157 (negative absolute vorticity) or $a < 0.0$ (maximum winds stronger than v_m) are not
158 allowed.

159 The iterative solution for the 13 coefficients of (2) follows this ad hoc steepest
160 descent procedure. Solutions were also found to be a function of which order the
161 variables were searched. In this work and in K07, the search order was a , θ , x , and
162 finally r_m . Variables were incremented up and down gradient in the following order, c_2 ,
163 c , γ , and finally v_m . Though we did not do a complete examination of the sensitivity to
164 search order, we did examine a few other search orders, and solving for the
165 asymmetries first provided larger asymmetries in the final solution and smaller errors
166 overall. The first guess sets all coefficients to zero, except m_o and x_o that are initialized

167 to the mean values of radius of maximum winds and the size parameter from the
168 western North Pacific sample (34 n mi, and 0.31). We did not use any other initial
169 conditions. Following this initial step, we increment the coefficients in Eq. 2, one at a
170 time, over a reasonable range of values (100 increments of 0.0005) to find the value of
171 the minimum mean square error vs best track wind radii. This new minimum becomes
172 the initial condition for the next iteration. We repeat the search, moving up and down
173 from the last minimum until we find convergence. Since the number of solutions to these
174 equations is very large, we choose only the set of model coefficients that is physically
175 consistent and near the global minimum in our loss function. Table 1 lists the final set of
176 solutions. For comparison, Table 1 also lists the original coefficients from K07 (their
177 Table 1), which were used in operations at JTWC, and the scaled versions from K07
178 (their Table 2).

179 The parametric vortex (1) with the parameters determined from the coefficients in
180 Table 1 defines the climatological part of the CLIPER model. Note the larger constant
181 for r_{mc} in the newly derived coefficients, and a much greater sensitivity of r_{mc} to both v_m
182 and γ . The operational model from K07, on the other hand, has very little asymmetry
183 (a_0 - a_3) and a fixed r_{mc} . Because the r_{mc} is a function of latitude in the new model, TC
184 that are more intense and at higher-latitude develop much larger circulations than either
185 version of coefficients given in K07. As a result, the new model should have larger
186 asymmetries that are dependent on both latitude and storm speed, which is consistent
187 with what we see in nature.

188 b. Persistence

189 Persistence is the second part of the model and is unchanged from what was done
 190 in K07 – a process described briefly here. Tropical cyclones can have both symmetric
 191 and asymmetric differences from the climatological model that can greatly influence the
 192 estimation of wind radii. Recall that the parameter x in our parametric model (1)
 193 represents the symmetric TC size. Using the observed wind radii and the climatological
 194 radius of maximum wind (r_{mc}), a value of x (x_{obs}) that provides the best fit to the
 195 symmetric mean of the observed radii (e.g., the average of NE, SE, SW and NW
 196 quadrants) is computed. This is done for each of the 34-, 50-, and 64-kt wind radii. The
 197 difference between x_{obs} and x_c is then defined as the initial symmetric error.

198 Then we use lag correlations of x_{obs} for the persistence. The lag correlations of the
 199 shape parameter x for our western North Pacific sample is shown in Figure 1. In this
 200 figure, the points are the observed lag correlations and the line is an approximation
 201 calculated as follows: First, we calculate the value of x_{obs} from the initial observations to
 202 capture the persistent nature of TC size. Then we apply the 12-hour basin-specific,
 203 linear regression coefficient and intercept to create a predicted value of x at 12 h

$$204 \quad x_{12} = x_c + [r_c (x_{obs} - x_c) + b_c] \quad (3)$$

205 In (3), x_c is the climatological value of x calculated using the forecast position and
 206 intensity at $t=12$ h, r_c is the regression coefficient and b_c is the intercept. In this sample,
 207 $r_c = 0.71$ and $b_c = -0.01$ at $t=12$ h. This calculation is repeated to estimate x at 24 to 120-
 208 h using the same values of r_c and b_c , where x_{obs} is replaced by the previous 12-h
 209 forecast. For example, the equation for 48 h is

$$210 \quad x_{48} = x_c + [r_c (x_{36} - x_c) + b_c] \quad (4)$$

211 In (4), x_c is the climatological value of x calculated using the 48-h forecast position and
212 intensity. Instead of the observed x , we now use the 36-h x (x_{36}) in the equation for 48 h.
213 This methodology approximates the points well as shown in Figure 1, but without the
214 added complication of carrying nine additional coefficients and intercepts.

215 To compute persistence of the asymmetric errors, we use the following strategy:
216 First, initial wind radii estimates are again used to calculate x_{obs} . Then x_{obs} is used in (1)
217 to predict wind radii in each quadrant at $t=0$. The differences between predicted and
218 observed wind radii in each quadrant are calculated and treated as initial errors in each
219 observed wind radii. At $t=0$ these errors are added back to the predicted values so that
220 the observed wind radii match the predicted wind radii at $t=0$. An e-folding time is used
221 to phase out the persistence of the asymmetric errors, and as in K07 this e-folding time
222 is set to 32 h. The initial errors effectively decay exponentially with time, becoming less
223 than 5% of its initial value by 120 h.

224 c. Intensification

225 If the storm intensifies past critical wind radii thresholds during the forecast, the
226 model generates forecasts for wind radii for these higher wind speed thresholds. Initial
227 errors from the next lower wind radii threshold provide an estimate of the asymmetries
228 for the higher-threshold wind radii. For instance, the initial R34 asymmetries for a storm
229 that has maximum winds of 45 knots are used to add asymmetry to the predicted R50
230 when the TC is forecast to intensify to 50 kt. In this way, the higher-threshold wind radii
231 asymmetries are prescribed to be consistent with R34 asymmetries throughout the
232 intensification process, regardless of the initial intensity.

233

234 3. Discussion

235

236 This work provides an update to the vortex climatology of the wind radii CLIPER
237 model (ATCF technique name DRCL) for the western North Pacific. The original vortex
238 climatology discussed in K07 was too small and too symmetric, resulting in
239 unrealistically small wind radii. It is important to note that the DRCL model formulation
240 has not changed and DRCL forecasts are still a blend of initial wind radii conditions and
241 a climatological vortex that is a function of storm intensity, latitude, and the direction and
242 speed of motion. JTWC forecasters provide both the initial wind radii and forecasts of
243 future positions and intensities. The updated western North Pacific DRCL coefficients
244 are developed with average radii that are 20-35% larger than in the original operational
245 model. As a result, the forecast wind radii for the longer ranges (after 48 h) are
246 noticeably larger. The initial conditions provided by JTWC forecasters, however will
247 largely determine the 0 to 24 h forecasts of wind radii. Figure 2 shows a comparison of
248 independent 2016 DRCL forecasts using the older K07 climatology and the updated
249 climatology presented here. This figure shows that errors are similar, but the large
250 negative biases in the older K07 climatology are eliminated by using this new
251 climatology. R50 and R64 wind radii are purposely de-emphasized here as the best
252 track values are regressed from the subjectively determined R34 and intensity. It is felt
253 that a higher quality validation data set is required to properly derive and evaluate the
254 R50 and R64 performance of this model. However, users should know that the new
255 formulation generally results in larger R50 and R64 forecasts as well.

256 Beginning in 2014, a concerted effort involving several agencies was initiated to 1)
257 determine the fidelity of wind radii estimation and forecasting, and 2) develop tools and
258 guidance to aid forecasters with the initial estimates and forecasts of tropical cyclone
259 surface winds. Sampson et al. (2017), Sampson and Knaff (2015), and Knaff et al.
260 (2017) describe many of these efforts. Because of this effort, operators and
261 researchers should be aware that the JTWC wind radii are now generally larger, in both
262 the best tracks and in the real-time estimates used to initialize NWP models and other
263 applications. Prior to September 2017, the DRCL in operations at JTWC (developed in
264 K07) was derived with the real-time wind radii estimates made with little objective
265 guidance. The result was large negative wind radii biases at longer leads (as Figure 2
266 shows for the 2016 western North Pacific season) and initial gale force wind radii
267 forecasts (i.e., when the TC first exceeded 34 kt) that were inconsistent with new wind
268 radii guidance. Note that $t=0$ errors in Fig. 2 are the result of differences between wind
269 radii used for initialization (i.e., real-time estimates) and the values in the final best
270 tracks. The effort presented here and in prior work should address many of these
271 inconsistencies. Furthermore, coefficients developed within this work will be used for
272 the wind speed probability product (DeMaria et al. 2009; DeMaria et al. 2013) run using
273 JTWC forecasts, and thus should provide improvements to downstream products like
274 TC Conditions of Readiness (Sampson et al. 2012) and significant wave height
275 probability forecasts (Sampson et al. 2016). Finally, the development of the DRCL
276 model presented here can easily be extended to longer lead forecasts, if JTWC extends
277 their wind radii forecasts beyond 120 h.

278

279 *Acknowledgements:* This work was funded by the US Navy under contract #N00604-
280 16-P-3503 at the Cooperative Institute for Research in the Atmosphere and through
281 Office of Naval Research, Program Elements 0602435N. We would also like to thank
282 the two anonymous reviewer and the associate editor, Elizabeth Ritchie, for their
283 comments and suggestions. The views, opinions, and findings contained in this report
284 are those of the authors and should not be construed as an official National Oceanic
285 and Atmospheric Administration or U.S. Government position, policy, or decision.

286 **References:**

287 Debye, P., 1909: Näherungsformeln für die Zylinderfunktionen für große Werte des
288 Arguments und unbeschränkt veränderliche Werte des Index. *Mathematische*
289 *Annalen*, **67**, 535–558 (in German), doi: <https://doi.org/10.1007%2FBF01450097>.

290 DeMaria, M., J. A. Knaff, R. Knabb, C. Lauer, C. R. Sampson, and R. T. DeMaria, 2009:
291 A new method for estimating tropical cyclone wind speed probabilities. *Wea.*
292 *Forecast.*, **24**, 1573-1591.

293 DeMaria, M., and Coauthors, 2013: Improvements to the operational tropical cyclone
294 wind speed probability model. *Wea. Forecast.*, **28**, 586-602.

295 Demuth, J., M. DeMaria, and J. A. Knaff, 2006: Improvement of Advanced Microwave
296 Sounding Unit Tropical Cyclone Intensity and Size Estimation Algorithms, *J. Appl.*
297 *Meteorol. Climatol.* ,**45**, 1573–1581.

298 Klotz, B. W., and H. Y. Jiang, 2016: Global composites of surface wind speeds in
299 tropical cyclones based on a 12year scatterometer database. *Geophys. Res. Lett.*,
300 **43**, 10480-10488.

301 Knaff, J. A., C. Guard, J. Kossin, T. Marchok, B. Sampson, T. Smith, and N. Surgi,
302 2007a: Operational guidance and skill in forecasting structure change. *Sixth Int.*
303 *Workshop on Tropical Cyclones*, San José, Costa Rica, *WMO Tech. Doc. 1383*.
304 [Available online at <http://severe.worldweather.org/iwtc/>.]

305 Knaff, J. A., C. R. Sampson, M. DeMaria, T. P. Marchok, J. M. Gross, and C. J. McAdie,
306 2007b: Statistical tropical cyclone wind radii prediction using climatology and
307 persistence. *Wea. Forecast.*, **22**, 781-791.

308 Knaff, J. A., S. P. Longmore, and D. A. Molenaar, 2014: An objective satellite-based
309 tropical cyclone size climatology. *Journal of Climate*, **27**, 455-476.

310 Knaff, J. A., C. R. Sampson, and G. Chirokova, 2017: A global statistical-dynamical
311 tropical cyclone wind radii forecast scheme. *Wea. Forecast.*, **32**, 629-644.

312 Knaff, J. A., C. J. Slocum, K. D. Musgrave, C. R. Sampson, and B. R. Strahl, 2016:
313 Using routinely available information to estimate tropical cyclone wind structure.
314 *Mon. Wea. Rev.*, **144**, 1233-1247. doi: 10.1175/MWR-D-15-0267.1

315 Knaff, J. A., M. DeMaria, D. A. Molenaar, C. R. Sampson and M. G. Seybold, 2011: An
316 automated, objective, multi-satellite platform tropical cyclone surface wind
317 analysis. *J. of Applied Meteorology and Climatology*.**50**, 2149-2166. doi:
318 10.1175/2011JAMC2673.1

319 Knaff, J. A., S. P. Longmore, R. T. Demaria, and D. A. Molenaar, 2015: Improved
320 tropical-cyclone flight-level wind estimates using routine infrared satellite
321 reconnaissance. *J. Appl. Meteor. Clim.*, **54**, 463-478.

322 Merrill, R. T., 1984: A comparison of large and small tropical cyclones. *Mon. Wea. Rev.*,
323 **112**, 1408-1418.

324 Sampson, C. R., and A. J. Schrader, 2000: The automated tropical cyclone forecasting
325 system (version 3.2). *Bull. Amer. Meteor. Soc.*, **81**, 1231-1240.

326 Sampson, C. R., and J. A. Knaff, 2015: A consensus forecast for tropical cyclone gale
327 wind radii. *Wea. Forecast.*, **30**, 1397-1403.

328 Sampson, C. R., J. A. Hansen, P. A. Wittmann, J. A. Knaff, and A. Schumacher, 2016:
329 Wave probabilities consistent with official tropical cyclone forecasts. *Wea. Forecast.*,
330 **31**, 2035-2045.

331 Sampson, C. R., E. M. Fukada, J. A. Knaff, B. R. Strahl, M. J. Brennan, and T. Marchok,
332 2017: Tropical cyclone gale wind radii estimates for the western north pacific. *Wea.*
333 *Forecast.*, **32**, 1029-1040.

334 Sampson, C. R., and Coauthors, 2012: Objective guidance for use in setting tropical
335 cyclone conditions of readiness. *Wea. Forecast.*, **27**, 1052-1060.

336 Uhlhorn, E. W., B. W. Klotz, T. Vukicevic, P. D. Reasor, and R. F. Rogers, 2014:
337 Observed hurricane wind speed asymmetries and relationships to motion and
338 environmental shear. *Mon. Wea. Rev.*, **142**, 1290-1311.

339 Weatherford, C. L., and W. M. Gray, 1988: Typhoon structure as revealed by aircraft
340 reconnaissance .2. Structural variability. *Mon. Wea. Rev.*, **116**, 1044-1056.

341

342 Figure Captions:

343 **Figure 1.** Points represent the linear lag correlation coefficient for the relationship
344 between the initial size parameter x and the observed x for each forecast hour. The
345 curve is the approximation used by the parametric wind radii CLIPER based on the 12-h
346 intercept and lag correlation coefficient.

347

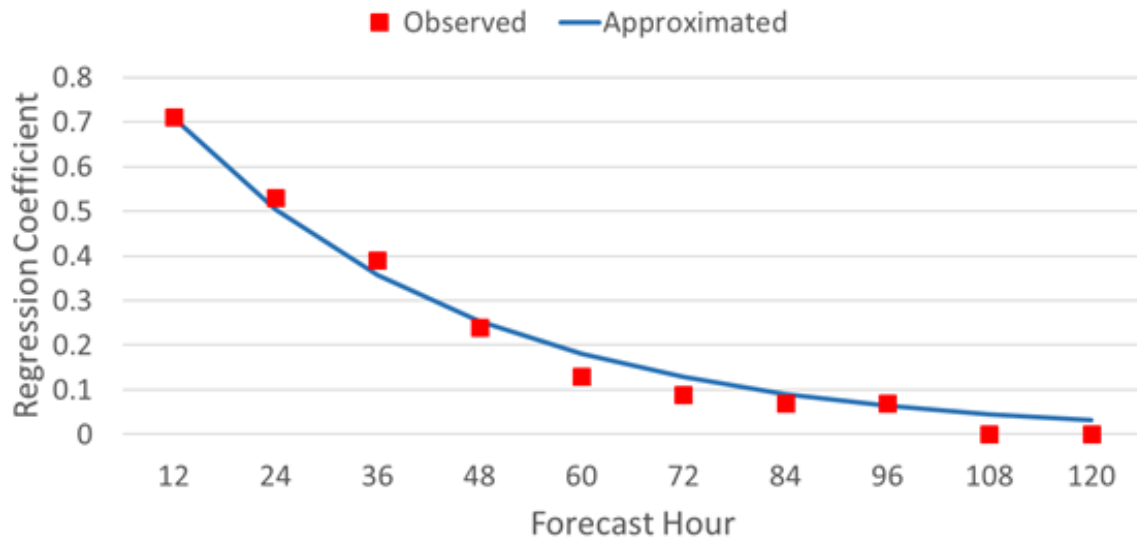
348 **Figure 2.** Old and newly recomputed DRCL mean forecast errors (solid) and biases
349 (dotted) for R34 using 2016 western North Pacific season JTWC best tracks as the
350 baseline. Cases for $t=0, 24, 48, 72, 96,$ and 120 h are 1353, 1510, 1185, 861, 588, and
351 380, respectively.

352

353 Table 1. Coefficients for Eq. 2 for the western North Pacific tropical cyclone basin used
 354 to create the climatological parametric wind radii CLIPER model. Coefficients from K07
 355 [operational (their Table 1) and derived using the scaling method (their Table 2)], and the
 356 new version developed in this effort. Units for the coefficients are shown in column 1.

	Western Pacific (K07, Table 1) Operational	Western Pacific (K07, Table 2) Scaling Method	Western Pacific (new)
t_0 [deg]	15.0000	14.4000	-13.0300
t_1	-0.5500	-0.0288	0.8485
t_2 [deg/kt]	1.0200	1.8000	1.0653
a_0 [kt]	0.6300	6.6800	4.2980
a_1	-0.0100	-0.1020	-0.1574
a_2 [kt ⁻¹]	0.0006	-0.0028	0.0035
a_3 [kt/deg]	-0.0300	0.1620	0.1276
x_0	-0.0059	0.2355	0.3151
x_1 [kt ⁻¹]	0.0055	0.0039	0.0038
x_2 [deg ⁻¹]	-0.0031	-0.0028	-0.0022
m_0 [n mi]	20.0000	38.0000	56.9200
m_1 [n mi/kt]	0.0000	-0.1167	-0.1541
m_2 [n mi/deg]	0.0000	0.0000	0.7372

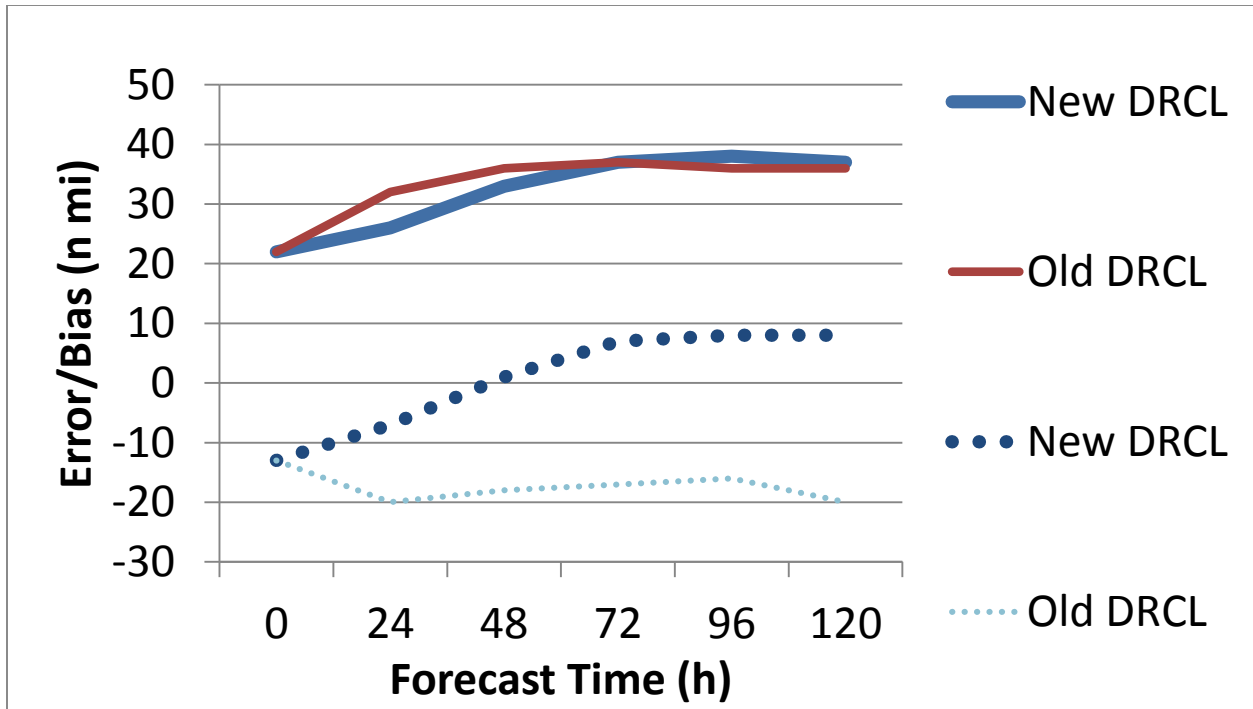
357



358

359 Figure 1. Points represent the linear lag correlation coefficient for the relationship
360 between the initial size parameter x and the observed x for each forecast hour. The
361 curve is the approximation used by the parametric wind radii CLIPER based on the 12-h
362 intercept and lag correlation coefficient.

363



364

365

366 Figure 2. Old and newly recomputed DRCL mean forecast errors (solid) and biases
 367 (dotted) for R34 using 2016 western North Pacific season JTWC best tracks as the
 368 baseline. Cases for $t=0, 24, 48, 72, 96,$ and 120 h are 1353, 1510, 1185, 861, 588, and
 369 380, respectively.

370

371